11802 *J. Phys. Chem. A* **2005,** *109,* 11802−11806

Empty Level Structure in Phenyl and Benzyl Isocyanates

Alberto Modelli*,[†,‡] and Derek Jones[§]

*Dipartimento di Chimica "G. Ciamician", Università di Bologna, via Selmi 2, 40126 Bologna, Italy;
Corso di Laurea in Scienze Ambientali, Piazza Kennedy 12, 48100 Ravenna, Italy; and ISOF,
Istituto per la Sintesi Organica e la Fotoreattività, C.N.R., via Gobetti 101, 40129 Bologna, Italy*

Received: September 23, 2005

The energies of the lowest-lying anion states of phenyl ($C_6H_5N{=}C{=}O$) and benzyl ($C_6H_5CH_2N{=}C{=}O$) isocyanates have been determined experimentally in the gas phase for the first time using electron transmission spectroscopy (ETS), and their localization properties have been evaluated using HF/6-31G, MP2/6-31G*, and B3LYP/6-31G* calculations. The lowest-lying anion state of phenyl isocyanate, mainly of benzene ring character but with some contribution also from the $N{=}C{=}O$ π-system, lies at significantly higher energy than that of other benzenes substituted by π-functionals, such as benzaldehyde or styrene. The scaling with the use of suitable empirical equations of the virtual orbital energies (VOEs) for orbitals with predominantly π^*_{ring} character calculated for the neutral-state molecules leads to vertical attachment energies (VAEs) which closely correspond to those determined experimentally, whereas those calculated for the predominantly π^*_{CO} and π^*_{NC} orbitals (3rd and 4th LUMO, respectively) are significantly different from the corresponding measured values notwithstanding the fact that the calculations reproduce the shortening of the $N{=}C$ and $C{=}O$ double bonds.

Introduction

Isocyanate (NCO) groups are of fundamental importance in the formation of polyurethanes through their reactions with alcohols.[1] They also react with other active hydrogen compounds such as amines, producing ureas, or with water, giving amines as the final product. With a suitable choice of monomers, photorefractive polyurethanes can be produced which offer interesting possibilities for a variety of important applications, including high-density optical data storage, image processing, and simulation of neural networks.[2,3]

In the silicon-based microelectronics industry, the specific reactivity of the isocyanate group allows the low-temperature production of highly controlled silicon oxide layers even down to monolayer levels.[4−7] The NCO group also reacts with silicon surface hydroxy groups, allowing the formation of molecularly ordered substrates[8] as well the production of luminescent organic−inorganic hybrid materials.[9]

Isocyanate-terminated prepolymers have been used to form ultrathin bio-compatible coatings[10] and organic NCO compounds react readily with surface hydroxyl groups on hydroxyapatite, thereby allowing its chemical grafting to organic polymers[11] in human bone reconstruction. The isocyanate group is also a highly reactive intermediate in surface catalytic reduction reactions, especially of NO_x emissions from internal combustion engines.[12]

In both the hydrolysis[13] and alcoholysis[14] of isocyanates, the addition reaction occurs in a concerted way across the $N{=}C$ bond of the isocyanate group rather than across the $C{=}O$ bond. The mechanisms are now known to be much more complex than a simple nucleophilic attack at the electron-deficient center on the NCO carbon atom, and data indicate that the N position is clearly favored for electrophilic attack with respect to the oxygen atom.

As a contribution toward a more fundamental understanding of this widely used and industrially important functional group, the present calculations and experimental data provide new electronic structure information in terms of the energies and localization properties of the lowest unoccupied electronic levels in phenyl and benzyl isocyanates.

Few experimental data have been reported in the literature on the electronic structure of isocyanates. The filled level structure, as determined by ultraviolet photoelectron spectroscopy, has been published[15] for $HC{=}N{=}O$ and its XH_3 derivatives (X = C, Si, Ge) and for phenyl isocyanate[16] ($C_6H_5N{=}C{=}O$) where the first two ionization events (9.00 and 9.62 eV) are associated with electron ejection from MOs with mainly benzene ring character. The same holds true for a series of ring-substituted phenyl isocyanate derivatives.[17] As far as the empty level structure is concerned, to our knowledge, no data are available.

In gas-phase collisions, an isolated molecule can temporarily attach an electron of proper energy and angular momentum into a vacant molecular orbital (MO), the process being referred to as a shape resonance.[18] Electron transmission spectroscopy (ETS)[19] is one of the most suitable means for detecting the formation of these unstable anion states. Because electron attachment is rapid with respect to nuclear motion, temporary anions are formed in the equilibrium geometry of the neutral molecule. The (positive) impact electron energies at which electron attachment occurs are properly denoted as vertical attachment energies (VAEs) and are the negative of the vertical electron affinities.

Within the Koopmans' theorem[20] (KT) approximation, VAEs are equal to the empty molecular orbital (MO) energies, just as the complementary ionization energies supplied by photoelectron

---

* Corresponding author. Tel: +39 051 2099522. Fax: +39 051 2099456. E-mail: alberto.modelli@unibo.it.

[†] Università di Bologna.

[‡] Corso di Laurea in Scienze Ambientali.

[§] ISOF, Istituto per la Sintesi Organica e la Fotoreattività, C.N.R.

10.1021/jp055420v CCC: $30.25

TABLE 1: Calculated Bond Distances (Å) and Angles (The geometrical parameters for the nearly coplanar conformer of benzylisocyanate are given in parentheses.)

		HF/6-31G	MP2/6-31G*	B3LYP/6-31G*	exptl
HN═C(*t*-Bu)$_2$	$d_{N=C}$	1.2685	1.2909	1.2786	
(CH$_3$)$_2$C═O[a]	$d_{C=O}$	1.2187	1.2276	1.2156	1.213
CH$_3$N═C═O[b]	d_{C-N}	1.4215	1.4446	1.4400	1.437
	$d_{N=C}$	1.1633	1.2161	1.2051	
	$d_{C=O}$	1.1916	1.1916	1.1817	
	∠CNC	179.99°	137.33°	139.86°	140.0°
	∠NCO	179.99°	172.10°	172.84	
PhN═C═O[c]	d_{C-N}	1.3823	1.4027	1.3985	1.370
	$d_{N=C}$	1.1658	1.2200	1.2090	1.207
	$d_{C=O}$	1.1877	1.1889	1.1787	1.171
	∠CNC	179.83°	137.76°	140.42°	140.6°
	∠NCO	179.95°	172.33°	172.99°	
PhCH$_2$NCO	d_{C-N}	1.4348 (1.4276)	1.4572 (1.4497)	1.4553 (1.4460)	
	$d_{N=C}$	1.1670 (1.1672)	1.2195 (1.2185)	1.2079 (1.2064)	
	$d_{C=O}$	1.1901 (1.1891)	1.1903 (1.1908)	1.1808 (1.1804)	
	∠CNC	166.25° (164.91°)	134.61° (136.21°)	137.83 (138.28°)	
	∠NCO	177.47° (177.36°)	172.27° (172.17°)	172.90° (173.14°)	
	dihedral C−C−N−C	89.71° (4.98°)	88.17° (32.47°)	87.51° (0.07°)	

[a] Experimental data from ref 33. [b] Experimental data from ref 34. [c] Experimental data from ref 35.

spectroscopy are equal to the negative of the energies of the filled MOs. ETS has thus proved a powerful means for elucidating the empty level electronic structure, as important as the filled counterpart from both the theoretical and reactivity points of view.

A theoretical approach adequate for describing the energetics of unstable anion states involves difficulties not encountered for neutral or cation states. The most correct approach is, in principle, the calculation of the total scattering cross section with the use of continuum functions, although complications arise when attempting to obtain an accurate description of the electron−molecule interactions.[21]

The first VAE can be obtained as the energy difference between the lowest-lying anion and the neutral state (both with the optimized geometry of the neutral species), but the description of resonance anion states (unstable with respect to electron loss) with standard bound state methods poses a serious problem. A proper description of the spatially diffuse electron distributions of anions requires a basis set with diffuse functions.[22,23] On the other hand, as the basis set is expanded, the wave function ultimately describes a neutral molecule and an unbound electron in as much of the continuum as the basis set can emulate,[24−27] since this is the state of minimum energy, thus not accounting for the fact that during a resonance process the extra electron is confined to the molecule by a potential barrier. The choice of a basis set which gives a satisfactory description of the energy and nature of resonance processes is therefore a delicate task.[28]

The Koopmans' theorem (KT) approximation neglects correlation and relaxation effects. However, Chen and Gallup[29] and Staley and Strnad[27] demonstrated the occurrence of good linear correlations between the $\pi^*_{C=C}$ VAEs measured in a large number of alkenes and benzenoid hydrocarbons and the corresponding virtual orbital energies (VOEs) of the neutral molecules obtained with simple KT-HF calculations, using basis sets which do not include diffuse functions. We have recently shown[24] that also the neutral state π^* VOEs obtained with B3LYP/6-31G* calculations supply a good linear correlation with the corresponding VAEs measured over a variety of different families of unsaturated compounds.

Here we analyze phenyl isocyanate $C_6H_5N{=}C{=}O$ and benzyl isocyanate $C_6H_5CH_2N{=}C{=}O$ (also labeled PhNCO and PhCH$_2$NCO in the text) by means of ETS for the first time and employ HF/6-31G, MP2/6-31G*, and B3LYP/6-31G* calculations to characterize the localization properties of the lowest-lying empty MOs of the neutral molecules and verify whether scaling of the π^* VOEs with appropriate empirical equations reported in the literature[27,24] can supply a good quantitative prediction of the corresponding measured VAEs also in these cumulated π-systems.

Experimental Section

Our electron transmission apparatus is in the format devised by Sanche and Schulz[19] and has been previously described.[30] To enhance the visibility of the sharp resonance structures, the impact energy of the electron beam is modulated with a small ac voltage, and the derivative of the electron current transmitted through the gas sample is measured directly by a synchronous lock-in amplifier. Each resonance is characterized by a minimum and a maximum in the derivative signal. The energy of the midpoint between these features is assigned to the VAE. The present spectra were obtained by using the apparatus in the "high-rejection" mode[31] and are, therefore, related to the nearly total scattering cross section. The electron beam resolution was about 50 meV (fwhm). The energy scale was calibrated with reference to the $(1s^12s^2)$ ^2S anion state of He. The estimated accuracy is ±0.05 or ±0.1 eV, depending on the number of decimal digits reported.

The calculations were performed with the Gaussian 98 suite of programs.[32] Geometry optimizations on the neutral molecules and evaluation of the virtual orbital energies are obtained at the Hartree−Fock (HF) level with the 6-31G basis set and at the MP2 and B3LYP level with the 6-31G* basis set.

Results and Discussion

Molecular Geometries. The geometries of the neutral molecules were optimized with HF/6-31G, MP2/6-31G*, and B3LYP/6-31G* calculations. Table 1 reports selected geometrical parameters for methyl, phenyl, and benzyl isocyanate and for the reference molecules HN═C(*tert*-butyl)$_2$ and (CH$_3$)$_2$C═O containing the noncumulated imine and carbonyl double bonds.

The geometrical factor which most directly affects the energy of the antibonding $\pi^*_{N=C}$ or $\pi^*_{C=O}$ MO is the double bond length. According to all three theoretical methods, the length of both the imine and the carbonyl double bonds (mainly the former) undergoes a sizable reduction on going from the noncumulated reference molecule to the isocyanates. On this

TABLE 2: Virtual Orbital Energies (VOEs), VOEs Scaled with Empirical Equations (in parentheses, see text), and Experimental VAEs[a]

	orbital	HF/6-31G	MP2/6-31G*	B3LYP/6-31G*	exptl VAE
C_6H_6[b]	b_{2g}	9.942 (5.01)	9.944 (5.01)	4.459 (4.80)	4.82
	e_{2u}	4.030 (1.15)	3.994 (1.16)	0.098 (1.29)	1.12
$(CH_3)_2C{=}O$[c]	π^*_{CO}	4.122 (1.21)	4.276 (1.34)	−0.303 (0.97)	1.31
$HN{=}C(t\text{-}Bu)_2$[d]	π^*_{NC}	4.741 (1.61)	4.696 (1.61)	0.291 (1.45)	1.29
$CH_3N{=}C{=}O$	$\pi^*_{NC}\text{-}n_O$	6.190 (2.56)	5.879 (2.38)	1.615 (2.51)	
	$\pi^*_{CO}\text{-}n_N$	6.190 (2.56)	4.821 (1.69)	0.658 (1.74)	
$PhN{=}C{=}O$	$\pi^*_O\text{-}\pi^*_{NC}\text{-}n_O$	10.095 (5.11)	10.056 (5.09)	4.546 (4.87)	4.87
0.658 (1.74)	$\pi^*_{NC}\text{-}n_O+\pi^*_O$	7.113 (3.16)	6.811 (2.98)	2.153 (2.95)	3.52
	$\pi^*_{CO}\text{-}n_N$	6.308 (2.64)	4.510 (1.49)	0.334 (1.48)	2.16
	π^*_A	3.424 (0.76)	3.508 (0.84)	−0.313 (0.96)	1.01
	$\pi^*_S+\pi^*_{NC}\text{-}n_O$	2.995 (0.48)	3.120 (0.59)	−0.631 (0.70)	0.58
$PhCH_2N{=}C{=}O$	π^*_O	9.587 (4.78)	9.661 (4.83)	4.427 (4.78)	4.43
	$p^*_{NC}\text{-}n_O$	6.306 (2.64)	6.384 (2.71)	1.992 (2.82)	≤3.4
perpendicular conformer	$\pi^*_{CO}\text{-}n_N$	5.827 (2.32)	5.053 (1.84)	0.755 (1.82)	2.5
	π^*_A	3.532 (0.83)	3.537 (0.86)	−0.287 (0.98)	
	π^*_S	3.365 (0.72)	3.369 (0.75)	−0.482 (0.82)	0.66

[a] All values in eV. [b] Experimental VAEs from ref 30. [c] Experimental VAEs from ref 36. [d] Experimental VAEs from ref 37.

SCHEME 1: Coplanar and Perpendicular Conformers of Benzyl Isocyanate

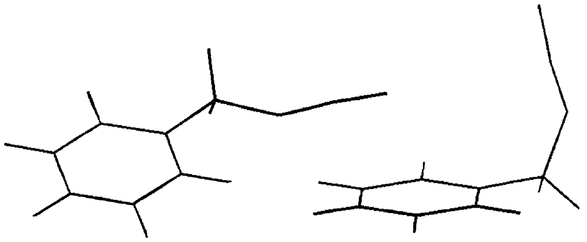

basis, the VAEs of the $\pi^*_{N=C}$ and $\pi^*_{C=O}$ MOs of the isocyanates are expected to be significantly higher than those of the corresponding MOs of the reference molecules.

The best agreement between the calculated geometrical parameters and the gas-phase experimental data (available for acetone,[33] methyl[34] isocyanate and phenyl[35] isocyanate, see Table 1) is obtained with the B3LYP/6-31G* calculations. In particular, the experimental value of about 140° for ∠CNC of methyl and phenyl isocyanate is reproduced closely and very closely, respectively, at the MP2 and B3LYP levels. In contrast, the HF/6-31G calculations largely fail, this angle being predicted to be close to 180°. As shown below, owing to the sensitivity of the $\pi^*_{C=O}$ MO energy to ∠CNC, this in turn leads to a sizable overestimation of the $\pi^*_{C=O}$ VAE supplied by the HF calculations with respect to the other two methods.

Finally, according to all three theoretical methods, in benzyl isocyanate there are two conformational minima, with the $C(H_2)-N$ single bond nearly perpendicular to or nearly coplanar with the ring plane (see Scheme 1). The perpendicular conformer is more stable, although the energy difference is small (within 0.3 ± 0.1 kcal/mol with all three methods). The geometrical parameters calculated for the coplanar conformer are reported in parentheses in Table 1.

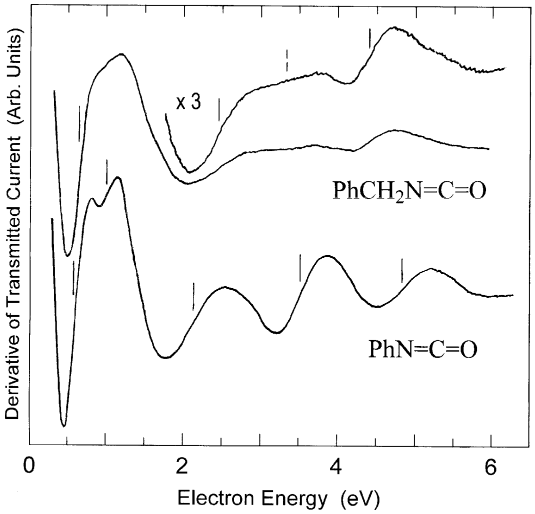

Figure 1. Derivative of transmitted current, as a function of the incident electron energy, in phenyl isocyanate and benzyl isocyanate. The vertical lines locate the VAEs.

ET Spectra and Empty Level Structure. PhNCO and $PhCH_2NCO$ possess five empty π^* MOs. Three of these derive from the benzene π^* MOs, that is, the degenerate (e_{2u}) LUMO and the totally antibonding (b_{2g}) MO (VAE = 1.12 and 4.82 eV, respectively[28]). The corresponding three MOs of the isocyanates with mainly ring character are labeled π^*_S, π^*_A, and π^*_O in Table 2. The remaining two cumulated π^*_{NC} and π^*_{CO} MOs lie in planes perpendicular to each other, so that they have the proper symmetry to mix, respectively, with the oxygen electron lone pair (n_O) and the nitrogen electron lone pair (n_N). The VAEs of the π^*_{NC} and π^*_{CO} MOs are 1.29 and 1.31 eV, respectively, in the reference molecules $HN{=}C(t\text{-}Bu)_2$[34] and $(CH_3)_2C{=}O$,[35] but the charge-transfer interactions with adjacent lone pairs are expected[38] to cause a sizable destabilization of the two π^* anion states in the isocyanates. In addition, as noted above, the reduction of the double-bond lengths acts in the same direction.

The ET spectra of phenyl and benzyl isocyanate, in the 0−6 eV energy range, are reported in Figure 1. The spectrum of PhNCO displays five distinct resonances. The first two are located at 0.58 and 1.01 eV, that is, at lower and slightly lower energy with respect to the π^* (e_{2u}) resonance of benzene (see Table 2). The latter value is likely to be considered an upper limit because the low-energy side of the second feature is partially superimposed upon the (more intense) first resonance. The third and fourth resonances are located at 2.16 and 3.52 eV. The fifth resonance (4.87 eV) occurs at the same energy (within experimental limits) as the π^* (b_{2g}) resonance of benzene.

Table 2 reports the π^* virtual orbital energies (VOEs) calculated for the neutral molecules with different methods for which good linear correlations between calculated π^* VOEs and corresponding experimental VAEs have been found and reported in the literature (HF/6-31G and MP2/6-31G*: ref 27; B3LYP/6-31G*: ref 24).

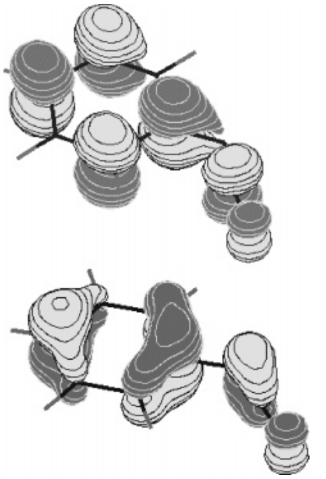

Figure 2. Representation of the HOMO and LUMO of phenyl isocyanate, as supplied by B3LYP/6-31G* calculations.

With all three methods, the first, second, and fifth VAEs of PhNCO, namely, those associated with electron attachment to the mainly benzene MOs, are well reproduced (within ±0.2 eV) by the scaled VOEs (given in parentheses in Table 2). Interaction with the mainly π^*_{NC} MO stabilizes the component (denoted π^*_S) of the benzene e_{2u} LUMO with maximum wave function coefficient at the substituted carbon atom, the perturbation experienced by the component (π^*_A) which possesses a node at the substituted carbon atom being much smaller. However, comparison with benzenes substituted with carbonyl or ethene π-functionals where the first anion state is stable (benzaldehyde, acetophenone[39]) or slightly unstable (styrene[40]) and the difference between the π^*_A and π^*_S VAEs is about 1 eV (vs 0.4 eV in PhNCO) reveals that the electron-acceptor properties of phenyl isocyanate are relatively poor and that its first anion state is mainly localized on the benzene ring, as confirmed by the localization properties calculated for the LUMO of the neutral molecule (see Figure 2).

The third and fourth resonances of the ET spectrum of PhNCO are unambiguously assigned by the calculations to the mainly π^*_{CO} MO (which lies in the plane of the σ-framework and is mixed in an antibonding manner with the nitrogen lone-pair n_N) and the mainly π^*_{NC} MO (mixed with the oxygen lone pair and the ring π-system), in order of increasing energy (see Table 2). In agreement with the above qualitative prediction, the π^*_{CO} and π^*_{NC} VAEs are 0.9 and 2.2 eV higher, respectively, than those of the separate reference molecules.

It is to be noticed, however, that the MP2 and B3LYP scaled VOEs underestimate the experimental π^*_{CO} (2.16 eV) and π^*_{NC} (3.52 eV) VAEs by 0.5−0.7 eV, a large error when compared with noncumulated π-systems such as alkenes and benzenoids,[24,27] mono- and diketones,[41] and pentacyclic heteroaromatics,[42] where the π^* VAEs are generally reproduced within ±0.2 eV.

The discrepancy (0.3 eV) between the π^*_{CO} and π^*_{NC} VAEs with the scaled VOEs supplied by the HF/6-31G calculations is smaller and, in addition, in the opposite direction for the π^*_{CO} VAE. However, this apparent better agreement with experiment can be traced back to a fortuitous compensation due to the above-mentioned failure of the HF/6-31G calculations in reproducing $\angle$CNC.

Figure 3 reports the scaled π^*_{CO} and π^*_{NC} VOEs of phenyl and benzyl isocyanate as a function of $\angle$CNC, allowing for optimization of all other geometrical parameters. The results obtained with the three methods are quite similar. In both compounds (mainly in PhNCO) the π^*_{CO} VAE is strongly dependent upon $\angle$CNC (the maximum π^*_{CO}/n_N overlap occurring at 180°), while the π^*_{NC} VAE increases with increasing $\angle$CNC is much less pronounced. This explains why the linear C−N−C arrangement erroneously predicted by the HF/6-31G calculations for PhNCO leads to a smaller underestimation of the π^*_{NC} VAE and to an overstimation of the π^*_{CO} VAE.

In $PhCH_2NCO$, the intermediate CH_2 group prevents mixing between the benzene and the N═C═O π-systems. In the perpendicular conformer, the degeneracy of the π^*_S and π^*_A MOs is removed by interaction of the former MO with the filled and empty σ-MOs localized at the $C(H_2)$−N bond (the σ-notation refers to the local symmetry). According to the calculations (see Table 2) the net resulting effect is a small stabilization (about 0.1 eV) of the π^*_S MO relative to π^*_A. In agreement, the ET spectrum displays a first resonance centered at 0.66 eV with an unresolved feature on the high-energy side. Mixing with the σ^*_{CN} MO seems to exert a larger effect on the π^*_O MO (stabilized by 0.4 eV with respect to the corresponding resonance in PhNCO and benzene), in line with the smaller energy gap between the interacting empty MOs.

Thus, the electron-acceptor properties of benzyl isocyanate are even smaller than those of phenyl isocyanate, and its first anion state even less localized on the N═C═O π-system.

The π^*_{CO} VAE (2.5 eV) of $PhCH_2NCO$ is higher than that of PhNCO, in line with a shorter length of the carbonyl double bond (see Table 1). The higher-lying π^*_{NC} resonance is partially overlapped and not well resolved from the π^*_{CO} resonance. The

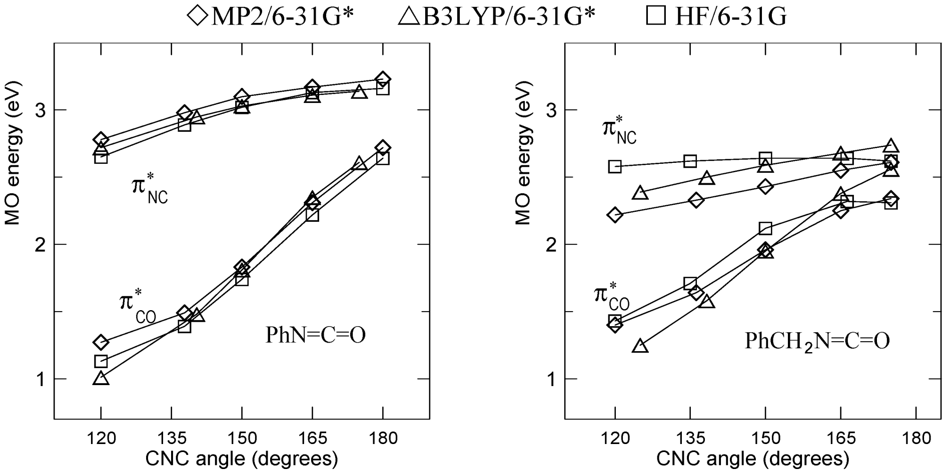

Figure 3. Scaled (see text) π^*_{CO} and π^*_{NC} VOEs calculated as a function of $\angle$CNC, allowing for optimization of all other parameters.

VAE of 3.4 eV located in Figure 1 is likely an upper limit. The absence of π^*_S/π^*_{NC} mixing (destabilizing for the latter MO) in benzyl isocyanate is in line with a smaller π^*_{NC} VAE than that of PhNCO. The scaled VOEs for benzyl isocyanate, as well as PhNCO, largely underestimate the π^*_{CO} and π^*_{NC} VAEs. The HF/6-31G scaled π^*_{CO} VOE closely approaches the corresponding measured VAE, but this is again due to an overestimation of $\angle$CNC (see Table 1).

Conclusions

The lowest-lying anion state of phenyl isocyanate is significantly more unstable than that of styrene or benzaldehyde, although there is a contribution not only from the ring but also from the N═C═O π-system. Moreover, the significant localization of the HOMO at the N atom and LUMO at the NCO carbon atom found here may be important in understanding the preference for the electrophilic/nucleophilic concerted attack which takes place across the N═C bond, rather than CO, during hydrolysis and alcoholysis reactions.

The reactivity of phenyl isocyanate cannot be explained in terms of its electron-acceptor properties; its electron affinity is in fact smaller than that of other benzenes substituted by π-functionals, and benzyl isocyanate possesses even poorer electron-acceptor properties than the phenyl compound.

Scaling with empirical equations of the π^*_{CO} and π^*_{NC} virtual orbital energies calculated for the neutral state molecules leads to VAEs which are significantly different from the corresponding measured values, notwithstanding the fact that the calculations reproduce the shortening of the double bonds in the isocyanates. This failure can be traced back to the fact that the empirical equations used in the literature are not calibrated for cumulative π-systems such as the isocyanates analyzed here.

Acknowledgment. A.M. thanks the Italian Ministero dell'Istruzione, dell'Università e della Ricerca, and the University of Bologna (Funds for Selected Topics) for financial support.

References and Notes

(1) Ulrich, H. *The Chemistry and Technology of Isocyanates*; Wiley: New York, 1996.

(2) Photorefractive Materials and their Applications I and II. *Topics in Applied Physics*; Günter, P., Huignard, J. P., Eds.; Springer-Verlag: New York, 1988; Vol. 61 and 62.

(3) Petrov, M. P.; Stepanov, S. I.; Khomenko, A. V. *Photorefractive Crystals in Coherent Optical Systems*; Springer-Verlag: New York, 1991.

(4) Uchida, Y.; Takei, S.; Matsumura, M. *Jpn. J. Appl. Phys., Part 1* **1996**, *35*, 1460.

(5) Fujimoto, A.; Sugiura, O. *Jpn. J. Appl. Phys., Part 1* **2000**, *39*, 5164.

(6) Taniguchi, H.; Sigiura, O. *Jpn. J. Appl. Phys., Part 2-Lett.* **1994**, *33*, L1485−L1488.

(7) Gasser, W.; Uchida, Y.; Matsumura, M. *Thin Solid Films* **1994**, *250*, 213.

(8) Jin, J. Y.; Johnstone, R. A. W. *J. Mater. Chem.* **1991**, *1*, 457.

(9) Li, H. R.; Lin, J.; Zhang, H. J.; Fu, L. S.; Meng, Q. G.; Wang, S. B. *Chem. Mater.* **2002**, *14*, 3651.

(10) Groll, J.; Ameringer, T.; Moeller, M.; Spatz, J. P. *Langmuir* **2005**, *21*, 1991.

(11) Liu, Q.; De Wijn, J. R.; Van Blitterswijk, C. A. *J. Biomed. Mater. Res.* **1998**, *40*, 358.

(12) Gao, H.; He, H. *Spectrochim. Acta, Part A* **2005**, *61*, 1233.

(13) Raspoet, G.; Nguyen, M. T.; McGarraghy, M.; Hegarty, A. F. *J. Org. Chem.* **1998**, *63*, 6867.

(14) Raspoet, G.; Nguyen, M. T.; McGarraghy, M.; Hegarty, A. F. *J. Org. Chem.* **1998**, *63*, 6878.

(15) Cradock, S.; Ebsworth, E. A. V.; Murdoch, J. D. *J. Chem. Soc., Faraday Trans. 2* **1972**, *68*, 86.

(16) Kobayashi, T.; Nagakura, S. *J. Electron Spectrosc. Relat. Phenom.* **1975**, *7*, 488.

(17) Novak, I.; Kovac, B. *J. Phys. Chem. A* **2003**, *107*, 2743.

(18) Schulz, G. J. *Rev. Mod. Phys.* **1973**, *45*, 378, 423.

(19) Sanche, L.; Schulz, G. J. *Phys. Rev. A* **1972**, *5*, 1672.

(20) Koopmans, T. *Physica (Amsterdam)* **1934**, *1*, 104.

(21) Lane, N. F. *Rev. Mod. Phys.* **1980**, *52*, 29.

(22) Hehre, W. J.; Radom, L.; Schleyer, P. v. R.; Pople, J. A. *Ab initio Molecular Orbital Theory*; Wiley: New York, 1986.

(23) Dunning, T. H., Jr.; Peterson, K. A.; Woon, D. E. *Basis Sets: Correlation Consistent Sets in the Encyclopedia of Computational Chemistry*; Schleyer, P. v. R., Ed.; John Wiley: Chichester, 1998.

(24) Modelli, A. *Phys. Chem. Chem. Phys.* **2003**, *5*, 2923.

(25) Guerra, M. *Chem. Phys. Lett.* **1990**, *167*, 315.

(26) Heinrich, N.; Koch, W.; Frenking, G. *Chem. Phys. Lett.* **1986**, *124*, 20.

(27) Staley, S. S.; Strnad, J. T. *J. Phys. Chem.* **1994**, *98*, 161.

(28) Modelli, A.; Hajgató, B.; Nixon, J. F.; Nyulászi, L. *J. Phys. Chem. A* **2004**, *108*, 7440.

(29) Chen, D. A.; Gallup, G. A. *J. Chem. Phys.* **1990**, *93*, 8893.

(30) Modelli, A.; Jones, D.; Distefano, G. *Chem. Phys. Lett.* **1982**, *86*, 434.

(31) Johnston, A. R.; Burrow, P. D. *J. Electron Spectrosc. Relat. Phenom.* **1982**, *25*, 119.

(32) Frisch, M. J.; Trucks, G. W.; Schlegel, H. B.; Scuseria, G. E.; Robb, M. A.; Cheeseman, J. R.; Zakrzewski, V. G.; Montgomery, J. A., Jr.; Stratmann, R. E.; Burant, J. C.; Dapprich, S.; Millam, J. M.; Daniels, A. D.; Kudin, K. N.; Strain, M. O.; Farkas, O.; Tomasi, J.; Barone, V.; Cossi, M.; Cammi, R.; Mennucci, B.; Pomelli, C.; Adamo, C.; Clifford, S.; Ochterski, J.; Petersson, G. A.; Ayala, P. Y.; Cui, Q.; Morokuma, K.; Malick, D. K.; Rabuck, A. D.; Raghavachari, K.; Foresman, J. B.; Cioslowski, J.; Ortiz, J. V.; Stefanov, B. B.; Liu, G.; Liashenko, A.; Piskorz, P.; Komaromi, I.; Gomperts, R.; Martin, R. L.; Fox, D. J.; Keith, T.; Al-Laham, M. A.; Peng, C. Y.; Nanayakkara, A.; Gonzalez, C.; Challacombe, M.; Gill, P. M. W.; Johnson, B.; Chen, W.; Wong, M. W.; Andres, J. L.; Head-Gordon, M.; Replogle, E. S. and Pople, J. A. *Gaussian 98*, Revision A.6; Gaussian, Inc.: Pittsburgh, PA, 1998.

(33) *Handbook of Chemistry and Physics*, 76th Ed.; Lide, D. R., Ed.; CRC Press: Boca Raton, New York, London, Tokyo, 1995−1996.

(34) Lett, R. G.; Flygare, W. H. *J. Chem. Phys.* **1967**, *47*, 4730.

(35) Bouchy A.; Roussy, G. *C. R. Acad. Sci. Paris C* **1973**, *277*, 143.

(36) Modelli, A.; Distefano, G.; Jones, D. *Chem. Phys.* **1982**, *73*, 395.

(37) Modelli, A.; Jones, D.; Rossini, S.; Distefano, G. *Tetrahedron* **1984**, *40*, 3257.

(38) Modelli, A. *Trends Chem. Phys.* **1997**, *6*, 57.

(39) Modelli, A.; Burrow, P. D. *J. Phys. Chem.* **1984**, *88*, 3550.

(40) Modelli, A.; Burrow, P. D. *J. Electron Spectrosc. Relat. Phenom.* **1983**, *32*, 263.

(41) Modelli, A.; Martin, H.-D. *J. Chem. Phys. A* **2002**, *106*, 7271.

(42) Modelli, A.; Burrow, P. D. *J. Phys. Chem. A* **2004**, *108*, 5721.